

1

2 **Supplementary Information for**
3 **Spin-triplet superconductivity from excitonic effect in doped insulators**
4 **Valentin Crépel and Liang Fu**
5 **E-mail: vcrepel@mit.edu, liangfu@mit.edu**

6 **This PDF file includes:**

- 7 Supplementary text
- 8 Figs. S1 to S2 (not allowed for Brief Reports)
- 9 SI References

10 Supporting Information Text

11 1. Effective model in the atomic limit

12 **A. General framework.** In this appendix, we derive the effective Hamiltonian used in the main text by treating the tunneling
13 terms

$$14 \quad \mathcal{H}_t = t_0 \sum_{\langle r,r' \rangle, \sigma} (c_{r,\sigma}^\dagger c_{r',\sigma} + hc), \quad [1]$$

15 as a perturbation to the 'classical' part $\mathcal{H}_0 = \mathcal{H} - \mathcal{H}_t$ (1), which is justified by the large gap $\Delta \gg t_0$. To that purpose, we
16 apply the unitary transformation $\mathcal{H}' = e^{iS} \mathcal{H} e^{-iS}$, with S Hermitian and satisfying (2)

$$17 \quad [\mathcal{H}_0, iS] = \mathcal{H}_t. \quad [2]$$

18 It leads to the following approximation of the Hamiltonian

$$19 \quad \mathcal{H}' = \mathcal{H}_0 + \frac{1}{2} [iS, \mathcal{H}_t] + \mathcal{O}(\mathcal{H}_t S^2), \quad [3]$$

20 obtained with the Baker-Campbell-Hausdorff formula. To find an explicit representation of S , we decompose the tunneling
21 Hamiltonian as

$$22 \quad \mathcal{H}_t = \sum_{d=\pm 1} \sum_{v=-5}^5 \sum_{u=-1}^1 T_{d,v,u}, \quad [4]$$

23 where $T_{d,v,u}$ gathers all tunneling events that change the number of occupied A sites by d , the number of nearest neighbor
24 pairs by v and the number of doubly occupied B -sites by u . In terms of these operators, we find

$$25 \quad S = -i \sum_{d,v,u} \frac{T_{d,v,u}}{d(\Delta_0 - U_A) + vV_0 + uU_B}. \quad [5]$$

26 Plugging this expression in Eq. 3, we obtain

$$27 \quad \mathcal{H}' = \mathcal{H}_0 + \frac{1}{2} \sum_{\substack{d,v,u \\ d',v',u'}} \frac{[T_{d',v',u'}, T_{d,v,u}]}{d'(\Delta_0 - U_A) + v'V_0 + u'U_B}, \quad [6]$$

28 which is valid up to $\mathcal{O}(t_0^3/\Delta^2)$ corrections.

29 **B. Projection.** The ground state of \mathcal{H}_0 for two electrons per unit cell has a singlet on all A -sites and B -sites completely empty.
30 Due to Pauli exclusion principle, the $x = n - 2$ doped electrons above this insulating state are placed at the B -sites. They have
31 an energy per particle $E_f = \Delta + 3V_0$. This low energy manifold, named f -band, hybridizes with local excitation having a hole
32 on a A -site due to the tunneling part \mathcal{H}_t . Such local excitation are separated from the low-energy band by an energy of at
33 least Δ . They are only virtually occupied due to the small ratio $t_0 \ll \Delta$, and their effects on the f -electrons' dynamics can be
34 obtained with Eq. 6.

35 Projecting \mathcal{H}' onto the f -band requires to have $d' = -d$ and $v' = -v$ in Eq. 6. Furthermore, the first operator acting on the
36 f -band should move an electron from an A to a B site, *i.e.* the rightmost $T_{d,v,u}$ must have $d = 1$ and $v, u \geq 0$. This gives

$$37 \quad \mathcal{H}' \simeq \mathcal{H}_0 - \frac{1}{2} \sum_{v,u,u' \geq 0} T_{-1,-u',-v} T_{1,u,v} \left[\frac{1}{\Delta_0 - U_A + vV_0 + uU_B} + \frac{1}{\Delta_0 - U_A + vV_0 + u'U_B} \right]. \quad [7]$$

38 This Hamiltonian can be recast as a tight binding Hamiltonian for the f -electrons on the triangular lattice, with density-assisted
39 hopping and local interactions:

$$40 \quad \mathcal{H}' = U_B \sum_{i \in B} \frac{n_i(n_i - 1)}{2} + \sum_{ijk \in \Delta} [\tilde{V}_{ij,k} + \circ_{ijk}] + \sum_{ijk \in \Delta, \sigma} [f_{j,\sigma}^\dagger \tilde{T}_{ij,k} f_{i,\sigma} + P_{ijk}], \quad [8]$$

41 where sums run over upper triangles with vertices ijk , while \circ_{ijk} and P_{ijk} respectively denote cyclic and all permutations of
42 ijk . The density dependent interaction and tunneling operators read

$$43 \quad \tilde{V}_{ij,k} = -\frac{t_0^2(2 - n_k)}{\Delta + (2 - n_\Delta)V_0 + n_k U_B}, \quad \tilde{T}_{ij,k} = \frac{t_{\Delta,i} + t_{\Delta,j}}{2}, \quad t_{\Delta,\ell} = \frac{t_0^2}{\Delta + (1 - n_\Delta)V_0 + n_\ell U_B}, \quad [9]$$

44 with $n_\Delta = n_i + n_j + n_k$, which are symmetric under the exchange $i \leftrightarrow j$. These interaction coefficients and density-dependent
45 tunneling amplitudes can be expressed in terms of sum and product of density operators. We now simplify their expression in
46 two particular cases.

47 **C. Dilute limit.** At small doping concentration, we can discard states with more than two fermions on the same triangle, which
 48 only appear with negligible probability. The tunneling coefficient $\tilde{T}_{ij,k}$ is thus restricted to cases where $(n_i + n_j = 0, n_k = 0)$,
 49 $(n_i + n_j = 1, n_k = 0)$ or $(n_i + n_j = 0, n_k = 1)$. Projecting on these configurations, we find the equivalent representation

$$50 \quad \tilde{T}_{ij,k} = T_{0,0} + n_k[T_{0,1} - T_{0,0}] + (n_i + n_j)[T_{1,0} - T_{0,0}]. \quad [10]$$

51 Summing over all possible triangle, we can rewrite

$$52 \quad \sum_{ijk \in \Delta, \sigma} [f_{j,\sigma}^\dagger \tilde{T}_{ij,k} f_{i,\sigma} + P_{ijk}] = \sum_{(i,j), \sigma} [f_{j,\sigma}^\dagger \left[t + \tilde{t} \frac{n_i + n_j}{2} \right] f_{i,\sigma} + hc] + \lambda \sum_{ijk \in \Delta, \sigma} [f_{j,\sigma}^\dagger n_k f_{i,\sigma} + P_{ijk}], \quad [11]$$

53 where we have introduced the coefficients

$$54 \quad t = \frac{t_0^2}{\Delta + V_0}, \quad \tilde{t} = \frac{t_0^2}{\Delta} + \frac{t_0^2}{\Delta + U_B} - \frac{2t_0^2}{\Delta + V_0}, \quad \lambda = \frac{t_0^2}{\Delta} - \frac{t_0^2}{\Delta + V_0}. \quad [12]$$

Similarly, we can project the interaction terms on configurations having $n_k, (n_i + n_j), (n_i + n_j + n_k) \leq 2$:

$$55 \quad \tilde{V}_{ij,k} = \tilde{V}_{ij,0} + n_k[\tilde{V}_{ij,1} - \tilde{V}_{ij,0}] + \frac{n_k(n_k - 1)}{2}[\tilde{V}_{0,0} - 2\tilde{V}_{0,1}] \quad [13]$$

$$= \tilde{V}_{0,0} + (n_i + n_j)[\tilde{V}_{1,0} - \tilde{V}_{0,0}] + \frac{n_i(n_i - 1) + n_j(n_j - 1) + 2n_i n_j}{2}[\tilde{V}_{2,0} - 2\tilde{V}_{1,0} + \tilde{V}_{0,0}] \quad [14]$$

$$+ n_k[\tilde{V}_{0,1} - \tilde{V}_{0,0} + (n_i + n_j)(\tilde{V}_{1,1} - \tilde{V}_{1,0} - \tilde{V}_{0,1} + \tilde{V}_{0,0})] + \frac{n_k(n_k - 1)}{2}[\tilde{V}_{0,0} - 2\tilde{V}_{0,1}].$$

56 Up to a global constant and a shift of chemical potential, this expansion leads to

$$57 \quad U_B \sum_{i \in B} \frac{n_i(n_i - 1)}{2} + \sum_{ijk \in \Delta} [\tilde{V}_{ij,k} + \odot_{ijk}] = U \sum_i \frac{n_i(n_i - 1)}{2} + V \sum_{(i,j)} n_i n_j, \quad [15]$$

58 where the coefficients read

$$59 \quad U = U_B + 3[2\tilde{V}_{2,0} - 4\tilde{V}_{1,0} - 2\tilde{V}_{0,1} + 3\tilde{V}_{0,0}], \quad V_f = \tilde{V}_{2,0} + 2\tilde{V}_{1,1} - 4\tilde{V}_{1,0} - 2\tilde{V}_{0,1} + 3\tilde{V}_{0,0}. \quad [16]$$

In terms of the lattice parameters t_0, Δ, V_0 and U_B , we find them equal to

$$60 \quad V = \frac{4t_0^2 V_0 (\Delta - V_0)}{\Delta(\Delta + V_0)(\Delta + 2V_0)} - \frac{2t_0^2 V_0}{(\Delta + U_B)(\Delta + V_0 + U_B)}, \quad U = U_B - \frac{6t_0^2 (4V_0^2 + V_0 \Delta + \Delta^2)}{\Delta(\Delta + V_0)(\Delta + 2V_0)} + \frac{6t_0^2}{\Delta + V_0 + U_B}. \quad [17]$$

61 Gathering the various terms, we obtain the expression given in the main text.

62 **D. Large U limit.** Assuming $U_B \gg t_0$, we can project the effective Hamiltonian to the f -band with no double occupancy.
 63 Restricting to $n_i \leq 1$ in the above equations yields the effective Hamiltonian

$$64 \quad \mathcal{H}' = \sum_{(i,j), \sigma} t (f_{i,\sigma}^\dagger f_{j,\sigma} + hc) + V n_i n_j + \sum_{(ijk) \in \Delta} \lambda \left(\sum_{\sigma} f_{i,\sigma}^\dagger n_k f_{j,\sigma} + P_{ijk} \right) + U_3 n_i n_j n_k, \quad [18]$$

65 where the coefficients t, λ and V have the same form as above. The three-body interaction terms read

$$66 \quad U_3 = \frac{12t_0^2 V_0^2}{\Delta(\Delta + V_0)(\Delta + 2V_0)} - \frac{6t_0^2 V_0^2}{(\Delta + U_B - V_0)(\Delta + U_B)(\Delta + V_0 + U_B)}. \quad [19]$$

67 2. Two-particle lattice calculation

68 In this appendix, we solve the effective model obtained above for two particles – the analog of Cooper's problem on the lattice.
 69 To do so, we separate the center of mass momentum K from the relative motion with the introduction of the states

$$70 \quad |\varphi_0(K, r)\rangle = \frac{1}{\sqrt{2(1 + \delta_{r,0})N_s}} \sum_R e^{i(K \cdot R)} (f_{R,\uparrow}^\dagger f_{R+r,\downarrow}^\dagger + f_{R+r,\uparrow}^\dagger f_{R,\downarrow}^\dagger), \quad |\varphi_1(K, r)\rangle = \frac{1}{\sqrt{N_s}} \sum_R e^{i(K \cdot R)} f_{R,\uparrow}^\dagger f_{R+r,\uparrow}^\dagger, \quad [20]$$

where the subscripts denotes the total spin S of the state (singlet $S = 0$ or triplet $S = 1$). The only difference between these spin configurations is their statistic under the exchange of the two particles, which translates into the sign difference $|\varphi_S(K, -r)\rangle = (-1)^S e^{i(K \cdot r)} |\varphi_S(K, r)\rangle$. The action of the Hamiltonian Eq. 18 on this basis is

$$71 \quad \begin{aligned} \mathcal{H}' |\varphi_S(K, r)\rangle &= \delta_{S,0} \delta_{r,0} U |\varphi_S(K, 0)\rangle + t \sum_{\substack{j=1,2,3 \\ \epsilon=\pm}} \delta_{r \neq 0} \delta_{r+\epsilon a_j \neq 0} [1 + e^{i\epsilon(K \cdot a_j)}] |\varphi_S(K, r + \epsilon a_j)\rangle \\ &+ \frac{\tilde{t}}{2} \sum_{\substack{j=1,2,3 \\ \epsilon=\pm}} \delta_{r, \epsilon a_j} [1 + e^{-i\epsilon(K \cdot a_j)}] \sqrt{2} |\varphi_S(K, 0)\rangle + \delta_{r,0} [1 + e^{i\epsilon(K \cdot a_j)}] \frac{1}{\sqrt{2}} |\varphi_S(K, \epsilon a_j)\rangle \\ &+ \sum_{\substack{j=1,2,3 \\ \epsilon=\pm}} \delta_{r, \epsilon a_j} [V |\varphi_S(K, \epsilon a_j)\rangle + \lambda |\varphi_S(K, -\epsilon a_j - \epsilon)\rangle] + \lambda \sum_{\substack{j=1,2,3 \\ \epsilon=\pm}} \delta_{r, \epsilon a_j} e^{i\epsilon(K \cdot a_j - \epsilon)} |\varphi_S(K, -\epsilon a_j + \epsilon)\rangle. \end{aligned} \quad [21]$$

71 We then solve this equation numerically for large enough system sizes to extract the ground state energy in each spin sector.
 72 Our solution are shown in the main text.

73 While our original model does not include any direct repulsion between B sites on the honeycomb lattice, the two-particle
 74 bound state we have established is robust against longer range interactions. To study their effect, we further add non-local
 75 interaction between conduction electrons to the effective Hamiltonian \mathcal{H}' and re-solve the two-particle problem. We find that
 76 bound state is destroyed only when the the non-local repulsion becomes comparable to the exciton-induced short-range pairing
 77 interaction (which is much larger than the binding energy ε_b). If we take into account the direct Coulomb repulsion between
 78 nearest-neighbor B sites V' , bound sate persists for $V' < 2\lambda - V$, or 0.25eV when the parameters mentioned in the main
 79 text are used. If we include the long-range Coulomb interaction $\frac{e^2}{\epsilon r}$ fully, bound state exists for $\epsilon a > 86.4\text{\AA}$ (a is the lattice
 80 constant), which corresponds to $e^2/\epsilon a = 16.5\text{meV}$. Thus, in order for electron pairing to occur in the limit of vanishing doping,
 81 it is helpful to have a large ϵ which can result from dielectric screening by a different band.

82 3. Continuum Limit

83 As shown in the main text, the kinetic part of the effective Hamiltonian dominates over interactions. Thus, low-energy fermions
 84 live near the two degenerate minima of the single-particle dispersion relation located at the K and K' points in the Brillouin
 85 Zone. Our goal here is to derive an effective continuum field theory capturing the physics of the system when fermions remain
 86 close to these two valleys.

87 We start with the momentum representation of the effective Hamiltonian \mathcal{H}'

$$88 \quad \mathcal{H}_f = \sum_{k,\sigma} \varepsilon_k f_{k,\sigma}^\dagger f_{k,\sigma} + \frac{1}{2N_s} \sum_{\substack{k,q,p \\ \sigma,\sigma'}} V_{k,q} f_{k,\sigma}^\dagger f_{q+p,\sigma'}^\dagger f_{k+p,\sigma'} f_{q,\sigma} \quad [22]$$

89 with N_s the number of unit cells in the lattice, $\varepsilon_k = 2t \sum_{j=1}^3 \cos(k \cdot a_j)$ and

$$90 \quad V_{k,q} = U + 2V \sum_j \cos[(k-q) \cdot a_j] + 2\lambda \sum_j (e^{ika_j + iq a_{j-1}} + e^{-ika_{j-1} - iq a_j}) + 2\tilde{t} \sum_j [\cos(k \cdot a_j) + \cos(q \cdot a_j)]. \quad [23]$$

91 Due to the quadratic band dispersion near the K and K' points, low energy fermions acquire an effective mass $m = 2/(3ta^2)$.
 92 They also carry an additional index $\{\uparrow K, \downarrow K, \uparrow K', \downarrow K'\}$ that distinguishes both their spin and their valley degeneracy and
 93 enable contact interactions between fermions with the same spin, provided they have opposite valley index.

94 Let us now focus on the scattering properties of these low energy fermions. Due to momentum conservation, two incoming
 95 low-energy fermions from the same valley can only scatter into a pair of fermions living in the same valley. The corresponding
 96 vertex interaction reads

$$97 \quad V_c = V_{K,K} = V_{K',K'} = 6(V - \lambda - \tilde{t}) + U. \quad [24]$$

98 When the electrons are in opposite valley K and K' , they can scatter to a pair in K and K' with the same valley preserving
 99 interaction strength V_c , or exchange valley to end up in K' and K through the vertex

$$100 \quad V_x = V_{K,K'} = V_{K',K} = 3(4\lambda - 2\tilde{t} - V) + U. \quad [25]$$

101 Introducing different fields for the two valleys

$$102 \quad f_{k,\sigma} = \begin{cases} \psi_{k,\sigma,K} & \text{if } k \text{ near } K \\ \psi_{k,\sigma,K'} & \text{if } k \text{ near } K' \end{cases}, \quad [26]$$

103 and accounting for the V_c and V_x terms, we find that the following effective interacting Hamiltonian

$$104 \quad \begin{aligned} \mathcal{H}_{\text{int}} = & \frac{V_c}{N_s} \sum_{\substack{k,q,p \\ V=K,K'}} \psi_{k,\uparrow,V}^\dagger \psi_{p-k,\downarrow,V}^\dagger \psi_{p-q,\downarrow,V} \psi_{q,\uparrow,V} + \frac{V_c - V_x}{N_s} \sum_{\substack{k,q,p \\ \sigma=\uparrow,\downarrow}} \psi_{k,\sigma,K}^\dagger \psi_{p-k,\sigma,K'}^\dagger \psi_{p-q,\sigma,K'} \psi_{q,\sigma,K} \\ & + \frac{V_c}{N_s} \sum_{\substack{k,q,p \\ V=K,K'}} \psi_{k,\uparrow,V}^\dagger \psi_{p-k,\downarrow,\bar{V}}^\dagger \psi_{p-q,\downarrow,\bar{V}} \psi_{q,\uparrow,V} + \frac{V_x}{N_s} \sum_{\substack{k,q,p \\ V=K,K'}} \psi_{k,\uparrow,V}^\dagger \psi_{p-k,\downarrow,\bar{V}}^\dagger \psi_{p-q,\downarrow,V} \psi_{q,\uparrow,\bar{V}}. \end{aligned} \quad [27]$$

105 Let us rearrange these terms in terms of pair operators to make their physical meaning clearer. Valley-polarized spin-singlet
 106 electron pairs $S_V = f_{V,\downarrow} f_{V,\uparrow}$ with $V = K, K'$ only feel the valley conserving term and therefore exhibit repulsive interaction
 107 ($V_c > 0$). When incoming electrons occupy opposite valleys, the ferromagnetic exchange leads to a total interaction strength
 108 $V_c + (-1)^S V_x$ depending on the total spin S of the pair. As a consequence, the last spin-singlet valley-triplet channel
 109 $S_0 = (f_{K',\downarrow} f_{K,\uparrow} - f_{K',\uparrow} f_{K,\downarrow})/\sqrt{2}$ is also repulsive ($V_c + V_x > 0$). On the contrary, the three valley-singlet spin-triplet pair
 110 states, $T_\sigma = f_{K',\sigma} f_{K,\sigma}$ with $\sigma = \uparrow, \downarrow$ and $T_0 = (f_{K',\downarrow} f_{K,\uparrow} + f_{K',\uparrow} f_{K,\downarrow})/\sqrt{2}$, all display a low-energy interaction strength

111 $V_c - V_x = 9(V - 2\lambda)$, which is negative for a wide range of parameter (see main text). To summarize, we can rewrite the
 112 different contact interaction terms as

$$113 \quad \tilde{H} = \int dx \sum_{\sigma,V} \psi_{\sigma,V}^\dagger \left[\frac{-\nabla^2}{2m} \right] \psi_{\sigma,V} + \int \frac{dx}{\mathcal{A}} [(V_c - V_x)(T_\downarrow^\dagger T_\downarrow + T_0^\dagger T_0 + T_\uparrow^\dagger T_\uparrow) + V_c(S_{K'}^\dagger S_{K'} + S_K^\dagger S_K) + (V_c + V_x)S_0^\dagger S_0], \quad [28]$$

114 with $\mathcal{A} = \sqrt{3}/a^2$ the Brillouin zone area. This effective field theory describes a four-component Fermi liquid with repulsive
 115 interactions in the spin-singlet channel, owing to the large on-site interaction U which appears in both V_c and in $(V_c + V_x)$, and
 116 attractive interaction between fermions with total spin one when $V_c - V_x < 0$.

117 Alternatively, we can replace pair operators by more physical quantities, such as the total density on each valley $\rho_V =$
 118 $\psi_{\uparrow,V}^\dagger \psi_{\uparrow,V} + \psi_{\downarrow,V}^\dagger \psi_{\downarrow,V}$ and the total spin on each valley $\mathbf{s}_V = \psi_{\alpha,V}^\dagger \boldsymbol{\sigma}_{\alpha,\beta} \psi_{\beta,V}$. Together, they allow to represent the exchange
 119 term as

$$120 \quad T_\downarrow^\dagger T_\downarrow + T_\uparrow^\dagger T_\uparrow + T_0^\dagger T_0 - S_0^\dagger S_0 = 2\mathbf{s}_K \cdot \mathbf{s}_{K'} + \frac{1}{2}\rho_K \rho_{K'}. \quad [29]$$

121 The valley conserving terms present in all interaction channels can be simply with the total density $\rho_{\text{tot}} = \rho_K + \rho_{K'}$

$$122 \quad T_\downarrow^\dagger T_\downarrow + T_\uparrow^\dagger T_\uparrow + T_0^\dagger T_0 + S_0^\dagger S_0 + S_K^\dagger S_K + S_{K'}^\dagger S_{K'} = \frac{1}{2}\rho_{\text{tot}}(\rho_{\text{tot}} - 1). \quad [30]$$

123 Together, they allow to rewrite the interaction part of the continuum Hamiltonian as

$$124 \quad \tilde{H}_i = \frac{1}{2\mathcal{A}} \int dx [V_c n_{\text{tot}}(n_{\text{tot}} - 1) - V_x (4\mathbf{s}_K \cdot \mathbf{s}_{K'} + n_K n_{K'})]. \quad [31]$$

125 This forms makes clear the ferromagnetic interactions between opposite valleys, which are responsible for the formation of
 126 triplet pairs. Expanding the total density as a function of ρ_K and $\rho_{K'}$, we find the three coupling constant given in the main
 127 text

$$128 \quad g_0 = V_c/(2\mathcal{A}), \quad g_1 = (2V_c - V_x)/(2\mathcal{A}), \quad g_2 = -2V_x/\mathcal{A}. \quad [32]$$

129 4. Mean-field theory of superconductivity

130 In this appendix, we carry out a mean-field treatment of the effective Hamiltonian Eq. 22 to investigate its superconducting
 131 behavior. With the mean-field substitution $f_{q',\sigma'} f_{q,\sigma} \simeq \delta_{q+q'} \langle f_{q',\sigma'} f_{q,\sigma} \rangle$, we get the following quadratic mean-field
 132 approximation:

$$133 \quad \mathcal{H}_{\text{mf}} = \sum_{k,\sigma} \xi_q f_{q,\sigma}^\dagger f_{q,\sigma} + \frac{1}{2} \sum_{k,\sigma,\sigma'} [\tilde{\Delta}_{k,\sigma\sigma'} f_{k,\sigma}^\dagger f_{-k,\sigma'}^\dagger + hc], \quad \tilde{\Delta}_{k,\sigma\sigma'} = -\frac{1}{N_s} \sum_q V_{k,q} \langle f_{q,\sigma} f_{-q,\sigma'} \rangle, \quad [33]$$

134 with $\xi_k = \xi_{-k} = \varepsilon_k - \mu$ and μ the chemical potential. It can be rewritten as a sum over a halved Brillouin Zone (denoted with
 135 primed sums and products below):

$$136 \quad \mathcal{H}_{\text{mf}} = \sum_k' [f_k^\dagger \quad f_{-k}] \begin{bmatrix} \xi_k & \Delta_k \\ \Delta_k^\dagger & -\xi_k \end{bmatrix} \begin{bmatrix} f_k \\ f_{-k}^\dagger \end{bmatrix}. \quad [34]$$

137 The order parameters have been gathered in a 2×2 matrix

$$138 \quad \Delta_k = \frac{\tilde{\Delta}_k - \tilde{\Delta}_{-k}^T}{2} = \frac{-1}{N_s} \sum_q \text{Re}(V_{k,q}) \langle f_{q,\sigma} f_{-q,\sigma'} \rangle, \quad [35]$$

139 and should be computed self-consistently.

140 **A. Pairing symmetries.** The explicit expression of $V_{k,q}$ allows to decompose this order parameter into spin-singlet and spin-triplet
 141 components

$$142 \quad \Delta_k = \Delta_s' + \sum_{j=1}^3 \Delta_j^s \cos(k \cdot a_j) + \Delta_j^t \sin(k \cdot a_j), \quad [36]$$

which respectively read:

$$\begin{aligned} \Delta_s' &= \frac{-1}{N_s} \sum_q [U + 2\tilde{t}(c_1 + c_2 + c_3)] \langle f_{q,\sigma} f_{-q,\sigma'} \rangle, \\ \Delta_j^s &= \frac{-2}{N_s} \sum_q [\lambda(c_{j-1} + c_{j+1}) + Vc_j + \tilde{t}] \langle f_{q,\sigma} f_{-q,\sigma'} \rangle, \\ \Delta_j^t &= \frac{2}{N_s} \sum_q [\lambda(s_{j-1} + s_{j+1}) - Vs_j] \langle f_{q,\sigma} f_{-q,\sigma'} \rangle, \end{aligned} \quad [37]$$

143 with $c_j = \cos(q \cdot a_j)$ and $s_j = \sin(q \cdot a_j)$. We can further split these order parameters in terms of irreducible representation of
 144 C_{3v} that they represent on the triangular lattice. For the singlet and triplet case, there are two one-dimensional irrep, only one
 145 of which can be obtained because of the particular form of $V_{k,q}$ and one two dimensional irrep. The two former measure the
 146 strength of s-wave and f-wave pairing

$$147 \quad \Delta'_s, \quad \Delta_{s/f} = \frac{1}{3} \left[\Delta_1^{s/t} + \Delta_2^{s/t} + \Delta_3^{s/t} \right], \quad [38]$$

148 while the two dimensional irrep are related to d-wave and p-wave pairing

$$149 \quad \Delta_{d_{x^2-y^2}/p_x} = \frac{1}{6} \left[\Delta_1^{s/t} + \Delta_2^{s/t} - 2\Delta_3^{s/t} \right], \quad \Delta_{d_{xy}/p_y} = \frac{1}{2} \left[\Delta_1^{s/t} - \Delta_2^{s/t} \right]. \quad [39]$$

150 The inverse transformations are

$$151 \quad \Delta_1 = \Delta_{s/f} + \Delta_{d_{x^2-y^2}/p_x} + \Delta_{d_{xy}/p_y}, \quad \Delta_2 = \Delta_{s/f} + \Delta_{d_{x^2-y^2}/p_x} - \Delta_{d_{xy}/p_y}, \quad \Delta_3 = \Delta_{s/f} - 2\Delta_{d_{x^2-y^2}/p_x}. \quad [40]$$

152 Finally, singlet pairs cannot be of equal spin, and we can therefore express them as a scalar times the 2×2 matrix $i\sigma_y$, *e.g.*
 153 $\Delta_s = d_0(i\sigma_y)$ with d_s a complex number. Triplet on the other hand, take the form of a Pauli vector multiplied by $i\sigma_y$, *e.g.*
 154 $\Delta_f = (\mathbf{d}_f \cdot \boldsymbol{\sigma})(i\sigma_y)$.

Our mean-field treatment relies on the self-consistent computation of four scalars related to singlet pairing in s-wave (Δ_s , Δ'_s) and d-wave ($\Delta_{d_{x^2-y^2}}$, $\Delta_{d_{xy}}$), and three vectors describing f-wave (Δ_f) or p-wave (Δ_{p_x} , Δ_{p_y}) pairs. The corresponding self-consistent equations become

$$\begin{aligned} \Delta'_s &= \frac{-1}{N_s} \sum_q \left[U + 2\tilde{t}(c_1 + c_2 + c_3) \right] \langle f_{q,\sigma} f_{-q,\sigma'} \rangle, \\ \Delta_s &= \frac{-2}{N_s} \sum_q \left[\tilde{t} + \frac{2\lambda + V}{3}(c_1 + c_2 + c_3) \right] \langle f_{q,\sigma} f_{-q,\sigma'} \rangle, \\ \Delta_{p_x} &= \frac{-2(\lambda + V)}{N_s} \sum_q \frac{s_1 + s_2 - 2s_3}{6} \langle f_{q,\sigma} f_{-q,\sigma'} \rangle, \\ \Delta_{p_y} &= \frac{-2(\lambda + V)}{N_s} \sum_q \frac{s_1 - s_2}{2} \langle f_{q,\sigma} f_{-q,\sigma'} \rangle, \\ \Delta_{d_{x^2-y^2}} &= \frac{2(\lambda - V)}{N_s} \sum_q \frac{c_1 + c_2 - 2c_3}{6} \langle f_{q,\sigma} f_{-q,\sigma'} \rangle, \\ \Delta_{d_{xy}} &= \frac{2(\lambda - V)}{N_s} \sum_q \frac{c_1 - c_2}{2} \langle f_{q,\sigma} f_{-q,\sigma'} \rangle, \\ \Delta_f &= \frac{2(2\lambda - V)}{N_s} \sum_q \frac{s_1 + s_2 + s_3}{3} \langle f_{q,\sigma} f_{-q,\sigma'} \rangle. \end{aligned} \quad [41]$$

155 **B. Self-consistent conditions.** The mean field quadratic Hamiltonian can be diagonalized by a Bogoliubov transformation.
 156 Writing the hermitian matrix

$$157 \quad \Delta_q \Delta_q^\dagger = a_0 + \mathbf{a} \cdot \boldsymbol{\sigma} \quad [42]$$

158 as a Pauli vector, the eigen-energies read

$$159 \quad E_{q,\pm} = \sqrt{\xi_q^2 + a_0 \pm |\mathbf{a}|}. \quad [43]$$

160 The corresponding eigenvectors lead to the following expression for the anomalous correlators

$$161 \quad \langle f_q f_{-q}^T \rangle = \left[g_q^+ + g_q^- \frac{\mathbf{a} \cdot \boldsymbol{\sigma}}{|\mathbf{a}|} \right] \frac{\Delta_q}{2}, \quad [44]$$

162 with

$$163 \quad g_q^\pm = \frac{g(E_{q,+}) \pm g(E_{q,-})}{2}, \quad g(E) = \frac{\tanh(\beta E/2)}{E}. \quad [45]$$

164 When $\Delta_q \Delta_q^\dagger$ is simply proportional to the identity, for instance when pairing occurs for spin-singlet, $E_{q,+} = E_{q,-} = E_q$ and the
 165 previous expression simply becomes $\langle f_q f_{-q}^T \rangle = g(E_q) \Delta_q/2$.

166 **C. Critical temperature.** Solving the self-consistent relations of Eq. 41 with the help of Eq. 44 allows to determine the nature of
 167 the superconducting state. We now consider each pairing channel separately to check whether a superconducting phase can
 168 fully form.

169 **C.1. s-wave.** The possibility of an s-wave SC order can be ruled out because U is much larger than all the other terms scaling as
 170 t_0^2/Δ . The coupled gap equations for Δ_s and Δ'_s linearized near T_c read

$$171 \begin{bmatrix} \Delta'_s \\ \Delta_s \end{bmatrix} = \begin{bmatrix} UI_0 + 2\tilde{t}I_1 & UI_1 + 2\tilde{t}I_2 \\ 2\tilde{t}I_0 + \frac{2(2\lambda+V)}{3}I_1 & 2\tilde{t}I_1 + \frac{2(2\lambda+V)}{3}I_2 \end{bmatrix} \begin{bmatrix} \Delta'_s \\ \Delta_s \end{bmatrix}, \quad [46]$$

172 where $I_k = -\sum_q \tanh(\beta E_q/2)(c_1 + c_2 + c_3)^k/(2N_s E_q)$ and β the inverse temperature. The matrix in the previous equation
 173 must have at least one eigenvalue equal to one for the system to exhibit s-wave symmetry. However, to leading order in U , this
 174 requires to have

$$175 U \left[\frac{2(2\lambda+V)}{3}(I_0 I_2 - I_1^2) - I_0 \right] = 0. \quad [47]$$

176 This equation has no solution because $(-I_0) > 0$ has the same sign as $I_0 I_2 - I_1^2 > 0$ (we used Cauchy-Schwarz inequality for
 177 the last inequality). Thus, s-wave singlet pairing does not happen in our model. It could nevertheless appear for smaller ratios
 178 Δ/t_0 where our perturbation theory breaks down.

179 **C.2. p-wave.** The possibility of p-wave pairing can be ruled out as well. Indeed, let's assume a p-wave SC order and compute
 180 the critical temperature T_c of that state. Linearizing the gap equation, such that $\mathbf{a} \simeq \mathbf{0}$ and $E_{q,\pm} \simeq |\xi_q|$, we find the coupled
 181 equations

$$182 \begin{bmatrix} \Delta_{px} \\ \Delta_{py} \end{bmatrix} = -\frac{V+\lambda}{N_s} \sum_q \frac{\tanh(\beta E_q/2)}{E_q} \begin{bmatrix} (s_1 + s_2 - 2s_3)^2/6 & (s_1 + s_2 - 2s_3)(s_1 - s_2)/6 \\ (s_1 - s_2)(s_1 + s_2 - 2s_3)/2 & (s_1 - s_2)^2/2 \end{bmatrix} \begin{bmatrix} \Delta_{px} \\ \Delta_{py} \end{bmatrix}. \quad [48]$$

183 Noting that $E_q = |\xi_q|$ is C_3 invariant, while the off-diagonal terms of the equation are not, we can rewrite the diagonal terms as:

$$184 \frac{-6}{V+\lambda} = \frac{1}{N_s} \sum_q \frac{\tanh(\beta E_q/2)}{E_q} \sum_j (s_j - s_{j+1})^2, \quad [49]$$

185 which does not have any solution since the left and right hand sides have opposite signs since $V + \lambda > 0$.

186 **C.3. d- and f-wave.** We can similarly derive an implicit equation for the critical temperature in the d-wave channel

$$187 \frac{6}{\lambda - V} = \frac{1}{N_s} \sum_q \frac{\tanh(\beta E_q/2)}{E_q} \sum_j (c_j - c_{j+1})^2. \quad [50]$$

188 Contrary to p-wave pairing, $\lambda - V$ can be positive for U_B not too large and V_0/Δ large enough. The region where $\lambda > V$
 189 is explicitly shown in the main text. The two independent order parameters $\Delta_{d_{xy}}$ and $\Delta_{d_{x^2-y^2}}$ are shown in Fig. S1. They
 190 exhibits nodal lines crossing the corners of the Brillouin zone, leading to a nodal superconducting order parameter at low
 191 doping when time reversal symmetry is not explicitly broken.

192 Turning to f-wave pairing, we find the effective gap equation

$$193 \frac{3}{2\lambda - V} = \frac{1}{N_s} \sum_q (s_1 + s_2 + s_3)^2 \frac{\tanh(\beta E_q/2)}{E_q}. \quad [51]$$

194 As explained in the main text, $2\lambda > V$ for most choice of parameter, leading to a superconducting order with f-wave symmetry
 195 that we extensively study in the main text. The competition between f- and d-wave superconducting state in regions where
 196 both of them are allowed is also discussed in the main text. In our model, f-wave pairing strongly dominate, but additional
 197 terms in the Hamiltonian may work in favor of the d-wave paired state.

198 5. Weakly interacting regime

199 **A. Explicit unitary transformation.** We start by isolating the band mixing (or off-diagonal) interaction elements from the
 200 others $\mathcal{V} = \mathcal{V}_{\text{od}} + \mathcal{V}_{\text{d}}$. More explicitly, we write $\mathcal{V}_{\text{od}} = \frac{1}{N_s} \sum_{C(1234)} V_{43}^{21} \delta_{43}^{21} c_4^\dagger c_3^\dagger c_2 c_1$, with $C(1234)$ restricting the sum to terms
 201 satisfying either $b_1 b_2 b_3 b_4 = -1$, or having $b_1 = b_2$ and $b_3 = b_4$ with $b_1 \neq b_2$.

202 To eliminate these band mixing interaction terms, we use a Schrieffer-Wolff transformation $\mathcal{H}' = e^S \mathcal{H} e^{-S}$, with S anti-
 203 hermitian. This unitary transformation can be carried order by order in the small parameter $|\mathcal{V}|/\Delta$, and we write $S = S_1 + S_2 + \dots$
 204 with $S_n = \mathcal{O}(|\mathcal{V}|^n/\Delta^n)$. Requiring

$$205 [H_0, S_1] = \mathcal{V}_{\text{od}}, \quad [52]$$

206 gets rid of the direct band-mixing terms in \mathcal{H}' :

$$207 \mathcal{H}' = \mathcal{H} + [S, \mathcal{H}] + \frac{1}{2}[S, [S, \mathcal{H}]] + \mathcal{O}(S^2 \mathcal{H}) = \mathcal{H}_0 + \mathcal{V}_{\text{d}} + \left[S_1, \mathcal{V}_{\text{d}} + \frac{\mathcal{V}_{\text{od}}}{2} \right] + [S_2, H_0] + \mathcal{O}\left(\frac{|\mathcal{V}|^3}{\Delta^2}\right). \quad [53]$$

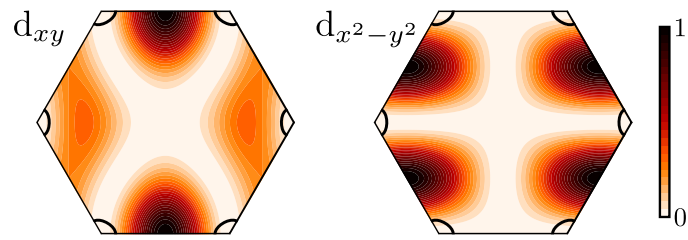


Fig. S1. Normalized d-wave superconducting order parameter amplitudes. The Fermi surface for $x = 0.1$ is indicated with a solid black line.

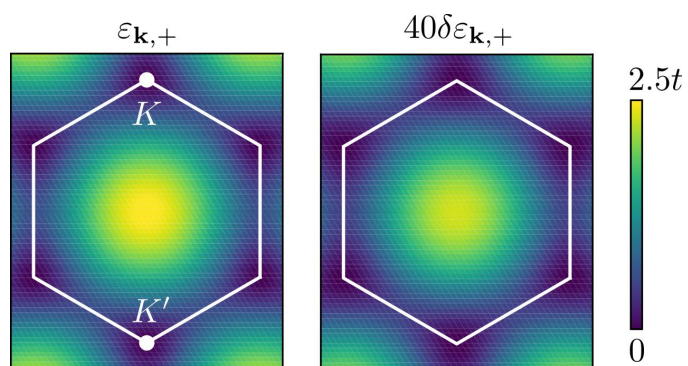


Fig. S2. Bare dispersion $\varepsilon_{\mathbf{k},+}$ and its leading correction $\delta\varepsilon_{\mathbf{k},+}$ (multiplied 40 times for visibility) in the weakly interacting limit, shown for $\Delta_0 = t = 2U_A = 2U_B = 10V_0$.

208 A possible S_1 satisfying this condition is

$$209 \quad S_1 = \sum_{C(1234)} \frac{V_{43}^{21} \delta_{43}^{21}}{\varepsilon_4 + \varepsilon_3 - \varepsilon_2 - \varepsilon_1} c_4^\dagger c_3^\dagger c_2 c_1. \quad [54]$$

210 We can then choose $[S_2, H_0]$ to remove the band mixing terms of $[S_1, \mathcal{V}_d + \mathcal{V}_{od}/2]$, and so on. Note that, because \mathcal{V}_d contains
211 no band mixing terms, such that $[S_1, \mathcal{V}_d]$ is purely off diagonal and therefore completely eliminated by $[S_2, H_0]$. The second
212 order corrections read $[S_1, \mathcal{V}_{od}]/2$, which as promised are of order $|\mathcal{V}|^2/\Delta$.

213 Finally, the effective Hamiltonian for doped charge is obtained by projecting \mathcal{H}' to the subspace where the lower band is
214 fully filled, which amounts to pairing up lower band indices as $c_a^\dagger c_b \rightarrow \tilde{\delta}_{a,b}$.

215 **B. Leading corrections.** To make analytical progress, we need the explicit form of the dispersion and scattering vertex. The
216 single particle energy dispersion reads

$$217 \quad \varepsilon_{\mathbf{k},\pm,\sigma} = \varepsilon_{\mathbf{k},\pm} = \pm \sqrt{(\Delta_0/2)^2 + |t_0 f(\mathbf{k})|^2}, \quad [55]$$

218 with $f(\mathbf{k}) = \sum_{j=1}^3 e^{i(\mathbf{k}\cdot\mathbf{u}_j)}$, and $\mathbf{u}_{j=1,2,3}$ the vectors connecting B sites to their three nearest neighbors. The corresponding
219 Bloch eigenvectors are

$$220 \quad \Psi_{\mathbf{k},\pm} = \frac{1}{\sqrt{2\varepsilon_{\mathbf{k},+}(\varepsilon_{\mathbf{k},+} \pm \Delta_0/2)}} \begin{bmatrix} \mp t_0 f(\mathbf{k}) \\ \varepsilon_{\mathbf{k},+} \pm \Delta_0/2 \end{bmatrix}, \quad [56]$$

221 They allow us to write the interaction vertex in the band basis as

$$222 \quad V_{43}^{21} = V_0 f(\mathbf{k}_4 - \mathbf{k}_1) [\Psi_{\mathbf{k}_4,b_4}^A \Psi_{\mathbf{k}_3,b_3}^B]^* \Psi_{\mathbf{k}_2,b_2}^B \Psi_{\mathbf{k}_1,b_1}^A + \sum_{\tau=A/B} \frac{U_\tau}{2} \delta_{(\sigma_4=\sigma_1)\neq(\sigma_3=\sigma_2)} [\Psi_{\mathbf{k}_4,b_4}^\tau \Psi_{\mathbf{k}_3,b_3}^\tau]^* \Psi_{\mathbf{k}_2,b_2}^\tau \Psi_{\mathbf{k}_1,b_1}^\tau. \quad [57]$$

223 The leading corrections to the band dispersion come from \mathcal{V}_d and are in the main text. The Hartree-like part takes the
224 explicit form

$$225 \quad \delta\varepsilon_{\mathbf{k},+}^H = (6V_0 C_- + U_A C_+) \frac{\varepsilon_{\mathbf{k},+} - \Delta_0/2}{2\varepsilon_{\mathbf{k},+}} + (6V_0 C_+ + U_B C_-) \frac{\varepsilon_{\mathbf{k},+} + \Delta_0/2}{2\varepsilon_{\mathbf{k},+}}, \quad [58]$$

226 with $C_\pm = (2N_s)^{-1} \sum_{\mathbf{q}} (\varepsilon_{\mathbf{q},+} \pm \Delta_0/2)/\varepsilon_{\mathbf{q},+}$. The Fock-like term reads

$$227 \quad \delta\varepsilon_{\mathbf{k},+}^F = \frac{t_0^2 V_0}{2N_s} \text{Re} \left[\frac{f^*(\mathbf{k})}{\varepsilon_{\mathbf{k},+}} \sum_{\mathbf{q}} f(\mathbf{k} - \mathbf{q}) \frac{f(\mathbf{q})}{\varepsilon_{\mathbf{q},+}} \right]. \quad [59]$$

228 These corrections are plotted together with the bare band dispersion for $\Delta_0 = t = 2U_A = 2U_B = 10V_0$ in Fig. S2, where we
229 observe that they both admit degenerate minima at the K and K' points.

230 When $t_0 \ll \Delta_0$, we can approximate $\varepsilon_{\mathbf{k},+} \simeq \Delta_0/2 + |t_0 f(\mathbf{k})|^2/\Delta_0$ and expand these corrections in powers of t_0/V_0 . Without
231 too much difficulty, we end up with

$$232 \quad \delta\varepsilon_{\mathbf{k},+}^H = \frac{|t_0 f(\mathbf{k})|^2}{\Delta_0^2} (U_A - 6V_0), \quad \delta\varepsilon_{\mathbf{k},+}^F = \frac{2t_0^2 V_0}{\Delta_0^2 N_s} \text{Re} \left[f^*(\mathbf{k}) \sum_{\mathbf{q}} f(\mathbf{k} - \mathbf{q}) f(\mathbf{q}) \right], \quad [60]$$

233 up to an overall global constant. These expressions allow to obtain the effective mass by expanding around the K or K' point.
234 For that purpose, we recall $f(K + \mathbf{k}) \simeq \sqrt{3}(k_x + ik_y)a/2$ and furthermore find that

$$235 \quad \sum_{\mathbf{q}} f(K + \mathbf{k} - \mathbf{q}) f(\mathbf{q}) = \sum_{\mathbf{q}} f(\mathbf{k} - \mathbf{q}) f(\mathbf{q} + K) \simeq \sum_{\mathbf{q}} f(-\mathbf{q}) f(\mathbf{q} + K) + \mathbf{k} \cdot \sum_{\mathbf{q}} (\nabla f)(-\mathbf{q}) f(\mathbf{q} + K) = 0 + \sqrt{3}(k_x + ik_y)a/2, \quad [61]$$

236 where the last equality is easy to check numerically. We end up with

$$237 \quad (\varepsilon + \delta\varepsilon^H + \delta\varepsilon^F)_{K+\mathbf{k},+} \simeq \frac{3t_0^2 a^2 |\mathbf{k}|^2}{4\Delta_0^2} (\Delta_0 + U_A - 4V_0), \quad [62]$$

238 yielding the effective mass given in the main text.

239 We now turn to the corrections to the two-body scattering vertex, which are contained in the second order term $X =$
240 $[S_1, \mathcal{V}_{od}]/2$. Direct evaluation of the commutator using the explicit expression of S_1 (Eq. 54) gives

$$241 \quad X = \frac{1}{N_s} \sum_{123456} \Gamma_{654}^{321} \delta_{654}^{321} c_6^\dagger c_5^\dagger (2c_4^\dagger c_3 - \delta_{3,4}) c_2 c_1, \quad [63]$$

242 where the indices 653 and 421 originates from the same interaction elements and thus satisfy the conditions given above for the
 243 elements of \mathcal{V}_{od} and S_1 . The three-body tensor Γ takes the form

$$244 \quad \Gamma_{654}^{321} = \frac{1}{N_s} \sum_0 \delta_{65}^{30} \delta_{40}^{21} (V_{65}^{03} - V_{65}^{30})(V_{04}^{21} - V_{40}^{21}) \left[\frac{1}{\varepsilon_6 + \varepsilon_5 - \varepsilon_3 - \varepsilon_0} + \frac{1}{\varepsilon_2 + \varepsilon_1 - \varepsilon_4 - \varepsilon_0} \right]. \quad [64]$$

245 For later use, we also define $\tilde{\Gamma}$ and $\hat{\Gamma}$, which have the same explicit representation except that the sum over 0 is restricted to
 246 states in lower band $b_0 = -$ and the upper band $b_0 = +$, respectively. To find the two-body corrections from X , we can select
 247 the terms where two of the indices belong to the lower band and contract them. Considering all possible pairs compatible with
 248 the constraints on 653 and 421, we end up with

$$249 \quad \delta V_{43}^{21} = 2 \sum_{i, b_i = -} \Gamma_{43i}^{i21} + \hat{\Gamma}_{i43}^{2i1} + \hat{\Gamma}_{i43}^{21i} + \hat{\Gamma}_{4i3}^{2i1} + \hat{\Gamma}_{4i3}^{21i} + 2 \sum_{i, b_i = -} \tilde{\Gamma}_{i43}^{i21} + \tilde{\Gamma}_{4i3}^{i21} + \tilde{\Gamma}_{43i}^{2i1} + \tilde{\Gamma}_{43i}^{21i} - \sum_i \tilde{\Gamma}_{43i}^{i21}. \quad [65]$$

250 This expression greatly simplifies when we assume that the four momenta $\mathbf{k}_{1,2,3,4}$ are equal to K or K' , as we do to determine
 251 the effective interaction strength in the spin-triplet valley singlet channel U_0 (see main text). Because $\Psi_{K/K',+}^A = 0$, any term
 252 of the form Γ_{654}^{321} with $6 = (K/K', +)$ or $1 = (K/K', +)$ appearing in U_0 vanishes (see Eq. 64). This completely removes any
 253 contribution from on-site interactions on A sites U_A . Let us first focus on the V_0^2 contributions and set $U_B = 0$ for a moment.
 254 This largely simplifies the expression of U_0 , which now reads

$$255 \quad U_0^{(1)} = 2 \sum_q \hat{\Gamma}_{(q-)(K+)(K'+)}^{(K'+)(K+)(q-)} + \hat{\Gamma}_{(q-)(K'+)(K+)}^{(K+)(K'+)(q-)} - \hat{\Gamma}_{(q-)(K+)(K'+)}^{(K+)(K'+)(q-)} - \hat{\Gamma}_{(q-)(K'+)(K+)}^{(K'+)(K+)(q-)}. \quad [66]$$

256 The two first terms of the sum involve interaction coefficients with momentum transfer K and K' , respectively, which makes
 257 them vanish as $f(K) = f(K') = 0$ (see Eq. 57). The other terms contribute equally, and we finally obtain

$$258 \quad U_0^{(1)} = -\frac{36t_0^2 V_0^2}{N_s} \sum_{\mathbf{q}} \frac{|f(\mathbf{q})|^2}{(2\varepsilon_{\mathbf{q},+})^3}. \quad [67]$$

259 It is not difficult to check that the contribution proportional to U_B^2 vanishes, and we now turn to the crossed $V_0 U_B$ corrections.
 260 The calculation proceeds in a similar way, except that one of the interaction element $3V_0$ is replaced by U_B and the signs needs
 261 to be flipped, such that the exchange part gives

$$262 \quad U_0^{(2)} = \frac{12t_0^2 V_0 U_B}{N_s} \sum_{\mathbf{q}} \frac{|f(\mathbf{q})|^2}{(2\varepsilon_{\mathbf{q},+})^3}. \quad [68]$$

263 For $t_0 \ll \Delta_0$, we use $\sum_{\mathbf{q}} |f(\mathbf{q})|^2 = 3N_s$ to find the simpler form

$$264 \quad U_0 = \frac{36t_0^2 V_0 (U_B - 3V_0)}{\Delta_0^3}, \quad [69]$$

265 which – remarkably – exactly match the result of the kinetic expansion in the weakly interacting regime

$$266 \quad U_0^{\text{KE}} = V_c - V_x \stackrel{(U_A, U_B, V_0 \ll \Delta_0)}{\simeq} \frac{36t_0^2 V_0 (U_B - 3V_0)}{\Delta_0^3}. \quad [70]$$

267 References

- 268 1. K Slagle, L Fu, Charge transfer excitations, pair density waves, and superconductivity in moiré materials. *Phys. Rev. B*
 269 **102**, 235423 (2020).
 270 2. JR Schrieffer, PA Wolff, Relation between the anderson and kondo hamiltonians. *Phys. Rev.* **149**, 491 (1966).